Activation-induced cytidine deaminase is dispensable for virus-mediated liver and skin tumor development in mouse models(Dissertation_全文)

AUTHOR(S):

Nguyen Manh Tung

OXFORD UNIVERSITY PRESS IntImm

Activation-induced cytidine deaminase is dispensable for virus-mediated liver and skin tumor development in mouse models

Journal:	*International Immunology*
Manuscript ID:	INTIMM-13-0213.R1
Manuscript Type:	Original Research
Date Submitted by the Author:	n/a
Complete List of Authors:	Nguyen, Tung; Graduate school of Medicine, Kyoto University, Immunology and Genomic Medicine Xu, Jianliang; Graduate school of Medicine, Kyoto University, Immunology and Genomic Medicine Chikuma, Shunsuke; Graduate school of Medicine, Kyoto University, Immunology and Genomic Medicine Hiai, Hiroshi; Graduate School of Medicine, Kyoto University, Medical Innovation Center Kinoshita, Kazuo; Shiga Medical Center Research Institute, Moriya, Kyoji; The University of Tokyo, Department of Infection Control and Prevention Koike, Kazuhiko; The University of Tokyo, Department of Gastroenterology Marcuzzi, Gian Paolo; University of Cologne, Institute of Virology and Center for Molecular Medicine Cologne Pfister, Herbert; University of Cologne, Institute of Virology and Center for Molecular Medicine Cologne Honjo, Tasuku; Graduate school of Medicine, Kyoto University, Immunology and Genomic Medicine Kobayashi, Maki; Graduate school of Medicine, Kyoto University, Immunology and Genomic Medicine
Keywords:	Hepatitis C Virus, Human Papillomavirus type 8, Activation-induced cytidine deaminase

(Title)
Activation-induced cytidine deaminase is dispensable for virus-mediated liver and skin tumor development in mouse models (106 letters)

(running title) AID is dispensable for virus-mediated oncogenesis (49 letters)

Tung Nguyen[1], Jianliang Xu[1], Shunsuke Chikuma[1], Hiroshi Hiai[2], Kazuo Kinoshita[3], Kyoji Moriya[4], Kazuhiko Koike[5], Gian Paolo Marcuzzi[6], Herbert Pfister[6], and Tasuku Honjo[1], Maki Kobayashi[1]

Affiliations
[1]Department of Immunology and Genomic Medicine and [2]Medical Innovation Center, Graduate School of Medicine, Kyoto University, Japan,
[3]Shiga Medical Center Research Institute, Japan,
[4]Department of Infection Control and Prevention, and [5] Department of Gastroenterology, The University of Tokyo, Japan,
[6]Institute of Virology and Center for Molecular Medicine Cologne, University of Cologne, Germany

606-8501, Yoshida-Konoe-cho, Sakyo-ku, Kyoto
honjo@mfour.med.kyoto-u.ac.jp
Tel +81 75 753 4371
Fax +81 75 753 4388

Total page number 45
5 Figures, 3 Tables, 3 Supplementary Figures and 4 Supplementary Tables

Keywords: Hepatitis C Virus, Human Papillomavirus type 8

Abstract

Activation–induced cytidine deaminase (AID) not only promotes immune diversity by initiating somatic hypermutation (SHM) and class switch recombination (CSR) in immunoglobulin (Ig) genes, but also provokes genomic instability by introducing translocations and mutations into non-Ig genes. To test whether AID is essential for virus-induced tumor development, we used two transgenic tumor models: mice expressing hepatitis C virus (HCV) core proteins (HCV-Tg) driven by the hepatitis B virus-promoter, and mice expressing human papillomavirus type 8 proteins (HPV8-Tg), driven by the Keratin 14 (K14) promoter. Both strains were analyzed in the absence and presence of AID by crossing each with *AID*$^{-/-}$ mice. There was no difference in the liver tumor frequency between the HCV-Tg/*AID*$^{+/+}$ and HCV-Tg/*AID*$^{-/-}$ mice at 20 months of age, although the *AID*$^{+/+}$ mice showed more severe histological findings and increased cytokine expression. Furthermore, a low level of AID transcript was detected in the HCV-Tg/*AID*$^{+/+}$ liver tissue that was not derived from hepatocytes themselves but from intra-hepatic immune cells. Although AID may not be the direct cause of HCV-induced oncogenesis, AID expressed in B cells, not in hepatocytes, may prolong steatosis and cause increased lymphocyte infiltration into HCV core-protein-induced liver lesions. Similarly, there was no difference in the time course of skin tumor

development between the HPV8-Tg/*AID*$^{-/-}$ and HPV8-Tg/*AID*$^{+/+}$ groups. In conclusion, AID does not appear to be required for tumor development in the two virus-induced tumor mouse models tested, although AID expressed in infiltrating B cells may promote inflammatory reactions in HCV core-protein-induced liver pathogenesis. (247 words)

Introduction

Activation-induced cytidine deaminase (AID) is essential for inducing DNA breaks during the somatic hypermutation and class switch recombination of immunoglobulin genes required for generating antibody diversity in activated B cells (1). AID generates physiological mutations during deliberate antibody development, but can also cause chromosomal translocations and mutations in proto-oncogenes when expressed aberrantly (2). Transgenic, ubiquitous over-expression of AID causes T cell lymphoma and micro-adenoma in the lung (3) along with mutations in the T cell receptor and c-myc genes. Chronic infections with micro-organisms such as helicobacter pylori (4), hepatitis C virus (HCV) (5-7), and human T cell leukemia virus type 1 (8) induce the aberrant AID expression, which has been proposed to cause tumors by introducing translocations and somatic mutations into proto-oncogenes. In addition, AID expression is associated with chronic infections of these pathogens in human cases, in which it has also been proposed to contribute to tumor formation at least in part (4, 9). However, it has not been directly determined if viral or bacterial-induced oncogenesis requires the action of AID.

Hepatocellular carcinoma (HCC) is the fifth most frequent cancer, and hepatitis B virus (HBV) and HCV infections are the major risk factors for developing this cancer worldwide (10). In fact the risk of developing

HCC is increased 11.5- to 17-fold in HCV-infected patients; however, antiviral therapies have limited effectiveness in only a small fraction of patients. Thus, elucidation of the mechanism(s) involved in promoting liver tumorigenesis is urgently required for developing a prevention strategy. As natural infection of HCV is restricted to humans and chimpanzees, several transgenic mouse models harboring parts of the HCV polyprotein have been generated to recapitulate HCC development (11). HCV, a small RNA virus, belongs to the Flaviviridae family and contains a 9.6-kb single-stranded RNA genome. The polyprotein encoded by the HCV genome is processed into the structural proteins including (core, E1 and E2) and the nonstructural proteins (NS2-NS5) required for RNA genome replication by host and viral proteases (11). Among them, the HCV core protein has unique, multifunctional roles in apoptosis, signal transduction, reactive oxygen species formation, transformation, and immune modulation (such as the up-regulation of TGF-β) (10), by interacting with many cellular proteins. Out of the 14 lines of HCV-transgenic mice developed, 5 HCV core protein-containing transgenic lines and one nonstructural (NS) 5A transgenic line can give rise to HCC, after the development of severe steatosis, a characteristic pathology associated with HCV infection (11-13). Especially, a transgenic mice model expressing HCV core protein (HCV-Tg) driven HBV regulatory elements (12) which limits HCV core

protein expression strictly in hepatocytes, had highest HCC prevalence among many HCV protein transgenic model mice (11, 13), therefore this model mice seemed to be a good tool to investigate AID expression in hepatocytes and its contribution to the mechanism of HCC development.

On the other hand, the human papillomavirus (HPV) family of small DNA tumor viruses, of which there are over 120 types, can cause hyper-proliferative lesions in cutaneous and mucosal epithelia (14). Among them, HPV5 and HPV8 are classified as high-risk beta-type papilloma viruses and are the two major causes of cutaneous squamous cell carcinoma (SCC) in epidermodysplasia verruciformis patients. The development of SCC by HPV8 is promoted by a series of carcinogenic events, including DNA damage, evasion of apoptosis, mutation mediated by E6 protein, and enhanced proliferation after ultraviolet light B exposure, mediated by E7 protein (14). Unlike HCV infection, HPV8 does not cause severe inflammation; however, DNA damage is an important carcinogenic process associated with this virus. A transgenic mouse model in which HPV8 early genes are expressed under the control of the Keratin 14 promoter (15) exhibits significant papilloma development (up to 91% of the HPV8-Tg mice) and malignant progression (6% of the HPV8-Tg mice back-crossed to FVB/N).

To determine whether AID is aberrantly induced by HCV or HPV8 and required for virally induced tumorigenesis, we crossed HCV-Tg or HPV8-Tg mice with *AID*$^{-/-}$ mice and compared the tumorigenesis frequencies in the *AID*$^{+/+}$ and *AID*$^{-/-}$ mice. We also examined the AID expression levels in the affected tissues. We found that HCV-Tg mice exhibited enhanced AID expression in the B cells infiltrating the liver, and that the steatosis and lymphocytic follicle formation were more severe in the HCV-Tg/*AID*$^{+/+}$ than in the HCV-Tg/*AID*$^{-/-}$ mice. However, the HCC prevalence at 20 months of age was not remarkably different between the two groups. Similarly, the time course of papilloma development was indistinguishable between the HPV8-Tg/*AID*$^{+/+}$ and HPV8-Tg/*AID*$^{-/-}$ mice. Furthermore, AID expression was not induced in the skin papillomatous tissues of the HPV8-Tg/*AID*$^{+/+}$ mice. We conclude that AID is not necessary for the viral protein-induced oncogenesis in these two mouse models.

Methods

Mice maintenance and genotyping

All the mice used in this study were maintained at the Institute of Laboratory Animals in accordance with the guidelines of the Animal Research Committee, Graduate School of Medicine, Kyoto University. *AID*$^{-/-}$ mice (16) back-crossed to C57/B6 (B6) were crossed with HCV core protein transgenic mouse line (HCV-Tg) (12, 13) and HPV8-Tg mice (on an FVB/N background) (15). AID-Cre and Rosa-RFP compound mice (17) were crossed with HCV-Tg mice to enable the detection of previous and current AID expression. The genotyping primers are described in Supplementary Table 1.

Western blotting

Western blotting was performed by conventional methods. Mouse organs were dissected and homogenized in RIPA buffer. The primary antibodies used were the rat monoclonal anti-mouse AID antibody 2 (MAID-2) (eBioscience, San Diego, USA), anti-Tubulin antibody (Calbiochem, MERCK, Darmstadt, Germany) and anti-HCV core protein antibody (clone B2, Yes Biotech Lab, Anogen, Ontario, Canada).

RT-PCR and qRT-PCR

Mouse organs were excised and homogenized in Sepasol RNA I Super (Nacalai Tesque, Kyoto, Japan) following the manufacturer's instructions.

RT-PCR was performed as previously described (18). ExTaq DNA polymerase (TaKaRa, Shiga, Japan) and the primers described in Supplementary Table 2 were used for conventional PCR. Real-time PCR was performed with the primer sets in Supplementary Table 2 and the Power SYBR Green PCR Master Mix (ABI, Life Technologies Japan, Tokyo, Japan) using the ABI 7900HT system (ABI). Delta-delta Ct method was used to calculate the fold change in gene expression. Error bars show the standard deviation.

Histology and immunohistochemistry

For AID immunohistochemical staining, freshly excised livers were fixed in 4% paraformaldehyde and processed for frozen section as previously described (19). AID protein was detected by MAID-2 and peroxidase-labeled donkey F(ab')2 anti-rat IgG (Jackson ImmunoResearch, West Grove, USA), and stained with Diaminobenzidine. Images were captured with a DM5000B microscope (Leica; Wetzlar, Germany). Hematoxylin and eosine (HE)-stained samples were fixed with Mildform 10N (Wako Pure Chemical Industries, Osaka, Japan), embedded in paraffin, and stained by standard methods.

Liver cell fractionation and FACS analysis

The isolation of intra-hepatic immune cells (IHICs) from the liver of HCV-Tg mice was performed as previously described, with some minor

modifications (20). The composition of IHIC cells was assessed by staining with the following antibodies: Phycoerythrin-labeled anti-mouse B220 for B cells, allophycocyanin (APC)-conjugated anti-mouse CD11b for Macrophages, and fluorescein isothiocyanate-labeled anti mouse CD8 and APC-anti mouse CD4 for T cells. The stained cells were analyzed on a FACSCalibur (BD Japan, Tokyo).

ELISA

TNF-α, IL-1β, and TGF-β were detected using ELISA kits specific for each cytokine (BioSource, Life Technologies), according to the manufacturer's instructions.

Statistical analysis

The Mann-Whitney U test was used to calculate the statistical differences in AID expression (Fig. 1B). Fisher's exact test was used to determine significant differences in tumor incidence (Table 3). Student's *t*-test was used to determine significant differences in cytokine expression (Fig. 3B and 3C), and Welch's *t*-test was used for pathological severity validation (Table 2). p values < 0.05 were considered statistically significant.

Results

Increased AID transcripts in the liver of HCV-Tg mice

To generate the observation groups, HCV-Tg mice were crossed with *AID*$^{-/-}$ mice. Then HCV-Tg/AID$^{+/-}$(HCV(+)AID$^{+/-}$) of the first filial generation was again crossed each other and the obtained HCV(+)AID$^{-/-}$ and HCV(+)AID$^{+/+}$ mice of the second filial generation were compared as the observation groups. The expression level of the HCV core protein in the liver was similar in the HCV(+)AID$^{-/-}$ and HCV(+)AID$^{+/+}$ mice (Supplementary Figure 1). Because HCV-Tg mice develop severe steato-hepatitis within 9 months after birth (12), and this chronic inflammation is supposed to reproduce the similar cytokine environment to the TNF-α-stimulated hepatocyte cell lines that express AID (9), we examined AID expression in the liver. AID transcripts were detected in the liver from 16-month-old HCV(+)AID$^{+/+}$ mice, but not from wild-type B6 mice (Fig. 1A, Supplementary Figure 2). However, the AID expression detected in the HCV(+)AID$^{+/+}$ liver was comparable to the low levels observed in primary un-stimulated spleen cells, which included B and T lymphocytes. Transcripts for CD19, a specific marker for B lymphocytes, were also higher in the HCV(+) compared to the B6 liver, suggesting that the HCV(+) liver may contain a considerable number of B lymphocytes,

which could contribute to the increased AID expression. Real-time PCR analysis revealed that the AID transcript level in the liver from 16 month-old HCV(+)AID$^{+/+}$ females was 15-fold greater than that from the liver of similarly aged B6 mice and of 12-month-old HCV(+)AID$^{+/+}$ males (Fig. 1B).

The AID protein levels were measured in the same liver samples by Western blotting (Fig. 1C). However, using the anti-mouse AID antibody 2 (MAID2), no protein signal could be detected in the same samples that contained AID transcripts (Fig. 1A). To quantify the limitation of AID protein detection by MAID2, we used spleen cells as a control (Supplementary Figure 3). We assigned one arbitrary unit of AID mRNA to the q-PCR signal detected from 500 ng of naïve spleen cell RNA. Extracts prepared from the same number of spleen cells contained 8.6 μg protein, which did not elicit a detectable AID signal in the Western blot. Since the AID transcript level from the HCV(+)AID$^{+/+}$ samples in Supplementary Figure 2 was lower than that in naive spleen cells, we conclude that the AID protein signal in the HCV(+)AID$^{+/+}$ liver was below the level detected by MAID2.

We next explored the possibility that the AID protein expression was limited to a specific location in the liver, such as the immune cells in the hepatic blood vessels. We therefore performed an

immunohistochemical analysis of AID (Fig. 1D). Although positive controls including liver tissue from CAG-promoter-driven AID transgenic mouse (3) and Peyer's patches from B6 wild type mouse showed clear brownish signals, there was no signal detected in any part of the HCV(+)AID$^{+/+}$ liver tissue samples.

AID transcripts are detected in intra-hepatic immune cells (IHICs), but not in hepatocytes from HCV-Tg mice.

We next explored the possibility that the low level of AID transcripts was contributed by B cells infiltrating the HCV-Tg liver. Liver cells from three HCV(+)AID$^{-/-}$ or HCV(+)AID$^{+/+}$ mice at 16 months of age were fractionated to separate the IHICs from the hepatocytes (Fig. 2A-B). RNA was purified from both fractions of each genotype, and the AID, CD19, and albumin transcripts were analyzed to confirm the purity of these fractions and to identify the cellular origin of the AID mRNA (Table 1). CD19 transcripts were detected almost exclusively in IHICs while albumin transcripts were mostly in hepatocytes, validating the fractionation procedure. The level of AID transcripts detected in the HCV(+)AID$^{+/+}$ IHICs was comparable to the level observed in splenic B cells (132.6±11.0 vs. 338.6±11.7, respectively), while the level in hepatocytes was much lower, indicating that the source of AID transcripts in the liver was not the

hepatocytes themselves but the IHICs. Cell surface marker analysis by FACS revealed that the IHICs consisted of $B220^+$ B cells (25-29%), $CD4^+$ or $CD8^+$ T cells (~45%), and $CD11b^+$ cells (7-10%), and that this composition was not notably changed by the presence of the HCV transgene or the AID genotype at 16 months of age (Fig. 2A, Supplementary Table 3).

To detect both current and past AID expression, transgenic reporter mice expressing tdRFP under the control of BAC-AID-Cre (17) were crossed to HCV-Tg mice (Fig. 2B, C, Supplementary Table 3). This mouse reveals tdRFP fluorescence in any cells that have (or had) expressed AID. Using this approach, $tdRFP^+$ cells were found to represent 3 to 4% of the total IHICs in both HCV-Tg and no HCV-Tg (HCV(-)) mice at 3 months of age (Fig. 2B). tdRFP was not detected in hepatocytes from 3-month-old HCV(+) mice that had already developed mild steatohepatitis (12). Analysis of 3 mice of each genotype (HCV(+) and HCV(–)) revealed that the tdRFP+ cells represented 5.8 ± 0.45 vs. $6.2 \pm 1.0\%$ of the B220+ population, respectively (Fig. 2C), indicating that the presence of the HCV transgene did not affect the AID gene expression in mice during the first 3 months of life.

AID deficiency reduces the severity of histopathological phenotypes and cytokine expression profiles in the liver of HCV-Tg mice

It is reported that 14-30% of HCV-Tg male mice develop HCC between 16 and 19 months of age (13). We therefore analyzed the histopathological phenotypes of HE-stained liver sections from HCV(+)AID$^{-/-}$ and HCV(+)AID$^{+/+}$ mice at 12 (male) and 16 (female) and 20 months (male) of age (Fig. 3A, 4A and Table 2). The severities of steatosis and lymphocyte infiltration were graded from 0 to 3, and the average scores for each group were calculated and tested by Welch's *t*-test (Table 2).

At 12 months of age, both HCV(+)AID$^{-/-}$ and HCV(+)AID$^{+/+}$ male mice had developed severe steatosis. Unexpectedly, the steatosis was milder in both HCV(+)AID$^{-/-}$ and HCV(+)AID$^{+/+}$ female mice at 16 months of age than HCV(+)AID$^{-/-}$ and HCV(+)AID$^{+/+}$ male mice at 12 months of age. The steatosis in the HCV(+)AID$^{+/+}$ mice appeared to be more severe than in HCV(+)AID$^{-/-}$ mice, but the difference was not significant (p>0.05). This decrease in steatosis severity may have been due to the female composition of the mice, because females of this HCV-Tg did not show tumor development (13) and human HCV infected cirrhotic females develop HCC less frequently (21). In addition, lymphoid follicle formation was apparent at 16 months of age and was more frequent in the HCV(+)AID$^{+/+}$ than the HCV(+)AID$^{-/-}$ mice (Fig. 3A, Table 2). Consistent

with the previous report (13), the fibrotic or regenerative nodular changes were very mild at 16 months of age.

However, the liver samples from both HCV(+)AID$^{-/-}$ and HCV(+)AID$^{+/+}$ mice at 20 months of age revealed marked progressive changes, with nuclear atypia detected in 10 out of 21 of each genotype, and liver cell degeneration or regenerative changes detected in 10 and 11 out of 21 HCV(+)AID$^{-/-}$ and HCV(+)AID$^{+/+}$ mice, respectively (Fig. 4A). Interestingly, both the steatosis and lymphoid follicle severity scores appeared to be higher in the HCV(+)AID$^{+/+}$ than the HCV(+)AID$^{-/-}$ 20-month-old mice (1.33 versus 1.00 for steatosis and 1.48 versus 1.14 for lymphoid follicles, respectively), although the observed differences were not statistically significant (Table 2).

We next examined whether the more advanced inflammatory histological phenotypes observed in the HCV(+)AID$^{+/+}$ mice were associated with increases in cytokine expression. Since cytokine production levels are altered in chronic HCV hepatitis (22) and in HCV-Tg mouse (23), we used q-PCR to measure representative pro-inflammatory Th1 and Th2 cytokine expression levels in the livers of 16-month-old female mice (Fig. 3B). The presence of the HCV transgene was associated with significantly higher levels of IL-1β, TNFα, and TGFβ mRNA, and HCV(+)AID$^{+/+}$ mice exhibited higher TNFα levels than HCV(+)AID$^{-/-}$ mice. Consistent with the

q-PCR results, the protein levels of IL-1β and TGFβ were also elevated by the presence of the HCV transgene, and TNFα protein production level was dependent on the presence of AID, suggesting that TNFα production may have led to the aggressive pathological findings observed in HCV(+)AID$^{+/+}$ mice (Fig. 3C).

Similar tumor incidence in HCV(+)AID$^{-/-}$ and HCV(+)AID$^{+/+}$ mice.

The incidence of tumor formation was carefully examined by histopathological and macroscopic evaluation. None of the 15 HCV(+)AID$^{-/-}$ or 15 HCV(+)AID$^{+/+}$ 16-month-old female mice showed evidence of liver tumor formation, consistent with a previous report (Table 3) (13). Further analysis of the 20-month-old male groups, including 21 HCV(+)AID$^{-/-}$ and 21 HCV(+)AID$^{+/+}$ mice, revealed that four out of 21 HCV(+)AID$^{+/+}$ mice carried macroscopic tumors, all of which were determined to be malignant by histological examination (Fig. 4A, right 4 panels). Similarly, three out of 21 HCV(+)AID$^{-/-}$ mice bore macroscopic tumors, two of which were judged to be malignant (Fig. 4A, left 3 panels). These results suggest that AID is not essential for HCV-induced carcinogenesis. Consistent with these findings, the AID transcript level in the tumor region of an AID$^{+/+}$ mouse (#241) was equivalent to the level detected in a non-tumor area (Fig. 4B). Comparison of the AID expression

in the tumor and non-tumor areas from the two tumor-bearing mice of the HCV(+)AID$^{-/-}$ and the two of HCV(+)AID$^{+/+}$ indicated that the tumor tissues did not contain elevated AID expression levels (Fig. 4C). The AID protein levels were not detectable by Western blotting in either the tumor or non-tumor areas (Fig. 4D).

Dispensability of AID for the development of skin tumors in HPV8-Tg mice

To examine AID's involvement in the development of HPV8-induced skin tumors, HPV8-Tg (HPV(+)) mice were crossed with AID$^{-/-}$ mice. Then HPV8(+)AID$^{+/-}$ of the first filial generation was again crossed each other and the obtained HPV8(+)AID$^{-/-}$ and HPV8(+)AID$^{+/+}$ mice of the second filial generation were compared as the observation groups. Both genotypes developed skin tumors, and tumor samples from 6-month-old mice were tested for AID expression by RNA and protein analyses (Fig. 5A, B). Neither the AID protein nor its RNA was detectable in the samples analyzed. After 6 months, the final skin tumor prevalence was ~30% in both mouse populations (15 out of 49 HPV8(+)AID$^{-/-}$ and 16 out of 51 HPV8(+)AID$^{+/+}$) (Supplementary Table 4), and the frequency and time course of tumor development in the 2 groups were almost indistinguishable (Fig. 5C). The histological examination of the skin tumor did not show any difference between HPV8(+)AID$^{+/+}$ and HPV8(+)AID$^{-/-}$ mice (Fig. 5D).

The lower papilloma prevalence (~30%) compared to the original report describing the HPV8(+) mice (15) may be due to the mixed genetic background of FVB/N and B6 in both groups (the HPV8(+)AID$^{-/-}$ and HPV8(+)AID$^{+/+}$ mice), since mice with an FVB/N genetic background are reported to have more severe papilloma progression than those with a B6 background (15). Although the malignant progression to SCC in these skin tumors was not examined, AID expression was absent, and tumor development was equivalent in the AID$^{-/-}$ and AID$^{+/+}$ mice. We thus conclude that AID is not involved in HPV8-induced skin tumorigenesis.

Discussion

In the current study, we investigated the requirement of AID for virally induced tumorigenesis by using compound mice that were generated by crossing mice transgenic for either HCV core proteins or HPV8 early proteins with either AID wild-type or knockout mice. Our results indicated that AID was expressed in neither hepatocytes of HCV-Tg nor skin tissue of HPV8-Tg. Thus AID was not shown to be required for the development of both HCV- and HPV8-promoted tumorigenesis. We could not conclude that the frequency of the liver malignancy is statistically different between HCV(+)AID$^{+/+}$ (4 out of 21 mice) and HCV(+)AID$^{-/-}$ (2 out of 21 mice), partly because the frequency of the liver malignancy was unexpectedly lower than that in the original report (13). Studies on 5 times number of mice may allow us to obtain statistically significant conclusion in the frequency of the liver malignancy between HCV(+)AID$^{+/+}$ and HCV(+)AID$^{-/-}$. We note, however, that the HCV(+)AID$^{+/+}$ mice exhibited higher levels of TNF-α production with more severe histological phenotypes than the HCV(+)AID$^{-/-}$ mice.

AID is reported to be expressed in HCC and in the surrounding non-cancerous liver tissues (6, 7). In addition, the hepatoma-derived cell lines HepG2, Hep3B, and Huh-7 have all been shown to express AID in response to HCV core protein-induced NF-κB signaling (9). It therefore

has been assumed that AID is induced in HCV-Tg mice and contributes to liver carcinogenesis. However, AID expression was not detected in HCV core protein-positive hepatocytes, and the low levels of AID transcripts in liver tissues were attributable to infiltrating B cells in the present study.

The different AID expression levels observed in the present mouse model and HCV-infected patients could be due in part to pathogenic differences between the two systems. HCV-Tg mice lack cirrhotic changes (12,13) which may be involved in inducing AID expression. In contrast, the natural course of human HCV infection leads to chronic hepatitis development, with bile duct damage and steatosis in the majority of patients (24), and the failure of virus eradication leads to liver cirrhosis and/or HCC (25). In human cases, 80-90% of the HCC develops from cirrhotic liver tissues (21), indicating that chronic inflammatory reactions generally contribute to carcinogenesis.

The involvement of B and T cells in liver injury by developing of autoimmune antibody may be a possible reason of strong inflammatory response in some part of the natural HCV infection cases (26, 27, 28). CD81, a HCV binding molecule is expressed on the surface of B and T cells and both lymphocytes may be infected by HCV (28,29). HCV infection to B cells causes non-organ specific autoantibodies (NOSAs) production and cryoglobulinemia (26, 30). In the various NOSAs, some

antibodies add autoantibody-mediated liver injury to viral hepatitis (30). For example, anti-liver/kidney microsomal antibody type 1 (LKM1) and anti-smooth muscle antibody (SMA) are also found in autoimmune hepatitis, and anti-microsomal antibody (AMA) is closely related to primary biliary cirrhosis (31). These liver-targeting antibodies of NOSAs are proposed to be produced based on the mimicry of the HCV polyprotein including NS3, 4 and 5 in addition to core, to autoantigens (32). In the current HCV-Tg mouse model, autoantibody-dependent liver injury is less likely because only core of the HCV polyprotein is expressed and HCV infection in B cells is absent. The absence of this extra-hepatic complication partly explains the reasons why the inflammation is weak in the present study compared to natural HCV infection and why AID is not expressed in the hepatocyte of HCV-Tg mouse.

The discrepancy of AID expression between the current animal study and the natural HCV infection could be also due to different regulation of AID expression between mouse and human hepatocytes. The transcriptional regulation of AID expression in B lymphocytes has been extensively examined both *in vitro* and *in vivo* and shown to depend on B cell-specific and environmental stimulus-specific factors (33). The latter include Stat6 and NF-κb, which are activated by viral infection. AID was activated by transfected HCV core protein responding to NF-κB signaling

pathway (9) in human cell lines, however, NF-κB is not activated in the current HCV-Tg model whereas up-stream TNF-α signal is increased (23). Although the difference in the AID promoter between human and mice is not known, we can not totally exclude this possibility to explain the different AID expression response.

Although HCV-Tg had weaker inflammatory responses than natural HCV infection, the inflammation observed in HCV(+)AID$^{+/+}$ mice tended to be more severe than that in HCV(+)AID$^{-/-}$ mice. The HCV core protein expression induced infiltration of IHICs including T, B and probably NK cells, and AID$^{+/+}$ B cells enhanced TNF-α production more than AID$^{-/-}$ B cells. The mechanism of TNF-α upregulation by AID is unknown, however, higher levels of TNF-α production is likely to affects the pathogenesis or prognosis. TNF-α and IL-1β were increased in the whole liver lysates of 16-month-old HCV-Tg mice, as previously reported (23). Clinically, increased TNF-α production from liver-infiltrating monocytes in Non-A, Non-B hepatitis has also been reported (34). Furthermore, TNF-α was shown to activate the AP-1 pathway (23), which promotes cell proliferation (35).

The HCC development without severe “cirrhotic” findings may be due to carcinogenic properties associated with the HCV core protein, including suppression of apoptosis (by interacting with p53 and pRb),

promotion of proliferation (by up-regulating the Wnt/b-catenin and Raf/MAPK pathways), and induction of reactive oxygen species (10, 36).

Stat3 is essential for HPV8-induced skin carcinogenesis (37). The Stat6 and Stat3 DNA recognition motifs are not completely identical, but share partial homology (38). We suspected that HPV8 induces AID through Stat and NF-κb signaling pathways, and examined AID's involvement in the HPV8-Tg mouse model. Contrary to our expectation, AID expression was not induced in the HPV8-Tg mouse model, which developed papilloma at a frequency of 30%. Since we observed these mice only up to 6 months before SCC development, we cannot rule out the possibility that AID in the skin squamous cells is induced later to convert papilloma to SCC.

In conclusion, our results suggest that AID may not be essential for either HCV-induced liver carcinogenesis or HPV8-induced papillomagenesis. We were unable to detect AID expression in transgenic cells expressing viral oncogenic proteins in either model, contrary to expectations. These results indicate that the expression of AID is strictly regulated in both hepatocytes and cutaneous keratinocytes at least in these mouse models used.

Abbreviations

Activation–induced cytidine deaminase (AID)

C57/B6 (B6)

CAG promoter-driven AID Tg (CAG-AID-Tg)

class switch recombination (CSR)

estrogen receptor (ER)

hepatitis B virus (HBV)

Hepatocellular carcinoma (HCC)

hepatitis C virus (HCV)

hepatitis C virus core protein transgenic mouse driven by the hepatitis B virus-promoter (HCV-Tg)

HCV-Tg (HCV(+))

no HCV-Tg (HCV(-))

Hematoxylin and eosine (HE)

the human papillomavirus (HPV)

human papillomavirus type 8 proteins transgenic mouse (HPV8-Tg)

HPV8-Tg (HPV8(+))

immunoglobulin (Ig)

intra-hepatic immune cells (IHICs)

Keratin14 (K14)

the rat monoclonal anti-mouse AID antibody 2 (MAID-2)

non-organ specific autoantibodies (NOSAs)

with reverse transcriptase (RT(+))

without reverse transcriptase (RT(-))

squamous cell carcinoma (SCC)

somatic hypermutation (SHM)

Acknowledgement

This work was supported by the Ministry of Education, Culture, Sports, Science and Technology of Japan Grant-in-Aid for Specially Promoted Research 17002015 (TH) and Grant-in-Aid for Scientific Research (C) 25440007 (MK). We thank Prof. Tsutomu Chiba for helpful discussions, Prof. Hitoshi Nagaoka for useful suggestions, Dr. Le Thi Huong for technical assistance, and Mrs. Mikiyo Nakata for providing HepG2 cells.

Table 1. AID, CD19, and Albumin mRNA levels in purified IHICs and hepatocytes

	CD19/18s rRNA			albumin/ 18s rRNA		AID/18s rRNA		
	IHICs	hepato-cytes	spleen B cells	IHICs	hepato-cytes	IHICs	hepato-cytes	spleen B cells
B6	326.6	3.3	920.0	1.0	1171.3	7.0 ± 0.30	1.0	338.6 ± 11.7
HCV(+)AID–/–	306.1	1.3		0.27	1082.0	0.0	0.0	
HCV(+)AID+/+	360.6	1.0		10.6	1027.2	132.6 ± 11.0	3.2 ± 0.63	

Relative AID/18s rRNA expression in B6 hepatocyte is set as 1.0, relative CD19/18s rRNA in HCV(+)AID+/+ as 1.0, and relative Albumin/18s rRNA in B6 as 1.0. Zero means undetectable signal by qPCR.

Table 2 The scored histological phenotypes of HCV(+)AID$^{-/-}$ and HCV(+)AID$^{+/+}$ mice

Steatosis in HCV(+)						
	Genotype	Severity score				
	of AID	0	1	2	3	Av.
12mo	–/–	0	0	0	3	3
	+/+	0	0	0	2	3
16mo	–/–	2	8	2	0	1.00
	+/+	0	8	4	0	1.33
20mo	–/–	9	7	1	4	1.00
	+/+	3	12	2	4	1.33
Lymphoid follicle in HCV(+)						
	Genotype	Severity score				
	of AID	0	1	2	3	Av.
16mo	–/–	9	3	0	0	0.25
	+/+	5	7	0	0	0.58
20mo	–/–	4	13	1	3	1.14
	+/+	2	11	4	4	1.48

The severity of steatosis and lymphoid follicle formation is classified as: 0 (none), 1 (mild), 2 (moderate), or 3 (severe). Values are the numbers of mice with each score. * AID$^{-/-}$ vs. AID$^{+/+}$, $p > 0.05$ by Welch's *t*-test.

Table 3 Liver tumor incidence in HCV-Tg mice

age	16 months		20 months	
AID genotype	-/-	+/+	-/-	+/+
male/female	0/15	0/15	21/0	21/0
Tumor	0	0	3	4
Malignancy	0	0	2	4*

*$AID^{-/-}$ vs. $AID^{+/+}$, $p > 0.05$ by Fisher's exact test.

References

(1) Honjo, T., Kinoshita, K., and Muramatsu, M. 2002. Molecular mechanism of class switch recombination: Linkage with somatic hypermutation. *Annu. Rev. Immunol.* 20:165.

(2) Nagaoka, H., Tran, T.H., Kobayashi, M., Aida, and M., Honjo, T. 2010. Preventing AID, a physiological mutator, from deleterious activation: regulation of the genomic instability that is associated with antibody diversity. *Int. Immunol.* 22:227.

(3) Okazaki, I.-M., Hiai, H., Kakazu, N. et al. 2003. Constitutive expression of AID leads to tumorigenesis. *J. Exp. Med.* 197:1173.

(4) Matsumoto, Y., Marusawa, H., Kinoshita, K. et al. 2006. *Helicobacter pylori* infection triggers aberrant expression of activation-induced cytidine deaminase in gastric epithelium. *Nat Med.* 13:470.

(5) Machida, K., Cheng, K. T.-N., Sung, V. M.-H. et al. 2004. Hepatitis C virus induces a mutator phenotype: Enhanced mutations of immunoglobulin and protooncogenes. *Proc. Natl. Acad. Sci. USA.* 101:4262

(6) Kou, T., Marusawa, H., Kinoshita, K. et al. 2006. Expression of activation-induced cytidine deaminase in human hepatocytes during hepatocarcinogenesis. *Int. J. Cancer.* 120:469.

(7) Vartanian, J-P., Henry, M., Marchio, A. et al. 2010. Massive APOBEC3 editing of hepatitis B viral DNA in cirrhosis. *Plos Pathog* 6: e1000928

(8) Ishikawa, C., Nakachi, S., Senba, M., Sugai M., and Mori N. 2011. Activation of AID by human T-cell leukemia virus Tax oncoprotein and the possible role of its constitutive expression in ATL genesis. *Carcinogenesis.* 32:110

(9) Endo, Y., Marusawa, H., Kinoshita, K. et al. 2007. Expression of activation-induced cytidine deaminase in human hepatocytes via NF-κB signaling. *Oncogene.* 26:5587.

(10) Tsai, W.-L. and Chung, R.T. Viral hepatocarcinogenesis. 2010. *Oncogene.* 29:2309.

(11) McGivern, D.R. and Lemon, S.M. 2011. Virus-specific mechanisms of carcinogenesis in hepatitis C virus associated liver cancer. *Oncogene.* 30:1969.

(12) Moriya, K., Yotsuyanagi, H., Shintani Y. et al. 1997. Hepatitis C virus core protein induces hepatic steatosis in transgenic mice. *J. Gen. Virol.* 78:1527.

(13) Moriya, K., Fujie, H., Shintani, Y. et al. 1998. The core protein of hepatitis C virus induces hepatocellular carcinoma in transgenic mice. *Nat. Med*. 4:1065

(14) Akgül B., Cooke, J. C. and Storey A. 2006. HPV-associated skin disease. *J Pathol.* 208:165.

(15) Schaper, I.D., Marcuzzi, G.P., Weissenborn, S.J. et al. 2005. Development of skin tumors in mice transgenic for early genes of human papilloma virus type 8. *Cancer Res.* 65:1394-1400.

(16) Muramatsu, M., Kinoshita, K., Fagarasoan, S., Yamada, S., Shinkai, Y. and Honjo, M. 2000. Class switch recombination and hypermutation require activation-induced cytidine deaminase (AID), a potential RNA editing enzyme. *Cell.* 102:553.

(17) Qin, H., Suzuki, K., Nakata, M. et al. 2011. Activation-induced cytidine deaminase expression in $CD4^+$ T cells is associated with a unique IL-10-producing subset that increases with age. *PLOS One.* 6:e29141.

(18) Kobayashi, M., Aida, M., Nagaoka, H., et al. 2009. AID-induced decrease in topoisomerase 1 induces DNA structural alteration and DNA cleavage for class switch recombination. *Proc Natl Sci USA.* 106:22375.

(19) Takai, A., Toyoshima, T., Uemura, M. et al. 2008. A novel mouse model of hepatocarginogenesis triggered by AID causing deleterious p53 mutations. *Oncogene.* 28:469.

(20) Blom, K.G., Rahman Qazi, M., Noronha Matos, J. B., Nelson, B. D., DePierre, J. W. and Abedi-Valugerdi M. 2008. Isolation of murine intrahepatic immune cells employing a modified procedure for mechanical disruption and functional characterization of the B, T and natural killer T cells obtained. *Clin. Exp. Immunol.* 155:320.

(21) Fattovich, I.G., Stroffolini, T., Zagni, I. and Donato, F. 2004. Hepatocellular carcinoma in cirrhosis: Incidence and risk factors. *Gastroenterology.* 127:S35.

(22) Castello, G., Scala, S., Palmieri, G., Curley, S.A., and Izzo, F. 2010. HCV-related hepatocellular carcinoma: From chronic inflammation to cancer. *Clin. Immunol.* 134:237.

(23) Tsutsumi, T., Suzuki, T., Moriya, K. et al. 2002. Alteration of intrahepatic cytokine expression and AP-1 activation in transgenic mice expressing hepatitis C virus core protein. *Virology.* 304:415.

(24) Bach, N., Thung S.N. and Schaffner F. 1992. The histological features of chronic hepatitis C and autoimmune chronic hepatitis: A comparative analysis. *Hepatology.* 15:572.

(25) World Health Org. (WHO). 2013. *Hepatitic C fact Sheet* No 164. Media Centre.

(26) Sansonno, D., Tucci, F.A., Lauletta, G. et al. 2006. Hepatitis C virus productive infection in mononuclear cells from patients with cryoglobulinemia. *Clin. Exp. Immunol.* 147:241.

(27) Himoto, T. and Nishioka, M. 2008. Autoantibodies in hepatits C virus-related chronic liver disease. *Hepatitis Monthly. 8*:295.

(28) Deng, J., Dekruyff, R.H., Freeman, G.J., Umetsu, D.T. and Levy, S. 2002. Critical Role of CD81 in cognate T-B cell interactions leading to Th2 responses. *Int. Immunol.* 14:513.

(29) Zhang, J., Randall, G., Higginbottom, A., Monk, P., Rice, C.M. and McKeating, J.A. 2004. CD81 is required for hepatitis C virus glycoprotein-mediated viral infection. *J. Virol.* 78:1448.

(30) Bogdanos, D.-P., Mieli-Vergani, G. and Vergani, D. 2005. Non-Organ-Specific autoantibodies in hepatits C virus infection: Do they matter? *Clin. Infect. Dis.* 40:508.

(31) Zeman, M.V. and Hirschfield, G.M. 2010. Autoantibodies and liver disease: Uses and abuses. *Can. J. Gastroenterol.* 24:225.

(32) Gregorio, G.V., Choudhuri, K., Ma, Y., et al. 2003. Mimicry between the hepatitis C virus polyprotein and antigenic targets of nuclear and

smooth muscle antibodies in chronic hepatitis C virus infection. *Clin Exp Immunol.* 133:404.

(33) Tran, T.H., Nakata, M., Suzuki, K. et al. 2010. B cell-specific and stimulation-responsive enhancers derepress *Aicda* by overcoming the effects of silencers. *Nat. Immunol.* 11:148.

(34) Yoshioka , K., Kakumu, S., Arao, A. et al. 1990. Immunohistochemical studies of intrahepatic tumour necrosis factor alpha in chronic liver disease. *J. Clin. Pathol.* 43:298.

(35) Shaulian, E. and Karin, M. 2001. AP-1 in cell proliferation and survival. *Oncogene.* 20:2390.

(36) Liang, T.J. and Heller, T. 2004. Pathogenesis of hepatitis C-associated hepatocellular carcinoma. *Gastroenterology.*127:S62.

(37) De Andrea, M., Rittà, M., Landini, M. M. et al. 2010. Keratinocyte-specific Stat3 heterozygosity impairs development of skin tumors in human papillomavirus 8 transgenic mice. *Cancer Res.* 70:7938.

(38) Ehret, G.B., Reichenbach, P., Schindler, U. et al. 2001. DNA binding specificity of different STAT proteins: Comparison of in vitro specificity with natural target sites. J. *Biol. Chem.* 276:6675.

Figure legends

Figure 1. AID expression in the liver of HCV-Tg mice. (A) Representative RT-PCR analysis showing AID mRNA expression in the liver of 16-month-old HCV(+)AID$^{+/+}$ mice. Naïve spleen RNA was included as a positive control. Numbers indicate individual mice. RT(+), with reverse transcriptase; RT(-), without reverse transcriptase. The arrow indicates primer-specific amplification and the arrowhead shows non-specific amplification. (B) Relative AID expression level in the liver of HCV(+)AID$^{+/+}$ mice at 16 months (n=15) and 12 months of age (n=7) and in wild-type (WT) 16 months-old (B6) mice (n=9), determined by quantitative (q) RT-PCR. *p* value by Mann-Whitney U test. (C) AID protein in the liver of the 16-month-old HCV-Tg mice analyzed in Fig. 1A, determined by Western blot. Splenocytes stimulated with IL-4 and LPS for three days were used as a positive control. (D) Immunohistochemistry for AID protein localization in the liver of HCV-Tg mice. The Peyer's patches and liver of a CAG-AID-Tg (CAG promoter-driven AID Tg) mouse were included as positive controls, and the liver of an AID$^{-/-}$ mouse was included as a negative control.

Figure 2. Cell surface marker analysis of intra-hepatic immune cells (IHICs) and hepatocytes from HCV-Tg mice. (A) Cell surface marker

profile of IHICs revealed by FACS analysis. The numbers indicate the percentage of each population. The data are representative of three independent experiments. (B) AID expression represented by the tdRFP reporter in the IHICs and hepatocytes from the liver of 3-month-old HCV(+)AIDcre/RFP and HCV(-)AIDcre/RFP mice. The FACS profile data shown in Fig. 2B and C are representative of 3 independent experiments. The definitive cell numbers of each quadrante in Figs.2B and 2C are shown in Supplementary Table 3. (C) Average percentage of $B220^{+}RFP^{+}$ cells in the $B220^{+}$ IHIC population from 3 independent experiments.

Figure 3. Inflammatory responses in the liver of HCV(+)AID$^{-/-}$ and HCV(+)AID$^{+/+}$ mice. (A) Representative liver histology shown by hematoxylin and eosin (HE) staining. Wild-type B6 mice (left panel), HCV(+)AID$^{-/-}$ (middle panel), and HCV(+)AID$^{+/+}$ (right panel) mice at 12 and 16 months of age (original magnification 200 ×). (B) mRNA expression of proinflammatory, Th1 and Th2 cytokines in the liver of 16-month-old mice. n=3 (mean ± SD). (C) ELISA detection of cytokines in whole liver lysates from 16-month-old wild-type B6, HCV(+)AID$^{-/-}$, and HCV(+)AID$^{+/+}$ mice. The data shown for each of the groups are based on the values from 6 mice, except for the IL1-β evaluation for the HCV(+)AID$^{+/+}$ group, which is based on 5 mice.

Figure 4. Development of hepatocellular carcinoma in HCV-Tg mice. (A) HE staining of the tumors found in HCV(+)AID$^{+/+}$ and HCV(+)AID $^{-/-}$ mice (original magnification 200×). (B) Representative AID mRNA expression profile in the tumor and non-tumor regions of HCV(+)AID$^{-/-}$ (#383) and HCV(+)AID$^{+/+}$ (#241) mice. (C) qRT-PCR of AID mRNAs analyzed as in Fig. 4B. Error bars show standard deviation from two mice of each group. (D) Western blot analysis of AID protein in samples from the same mice analyzed in Fig. 4B.

Figure 5. Cutaneous papilloma in HPV8(+)AID$^{-/-}$ and HPV8(+)AID$^{+/+}$ mice. (A) Representative results of the RT-PCR analysis of AID mRNA in skin tumors of HPV8(+)AID$^{-/-}$ (1, 2, 3) and HPV8(+)AID$^{+/+}$ (4, 5, 6) littermates, and a positive control (naïve spleens of HPV8(+)AID$^{+/+}$ mice). The data shown are representative of 3 independent experiments (n=9 for each group) (B) Representative results of Western blots detecting AID protein in lysates of skin tumors from HPV8(+)AID$^{+/+}$ mice. The negative control was skin tissue from HPV8-Tg negative AID$^{-/-}$, and the positive control was a lysate of spleen cells from HPV8(+)AID$^{+/+}$ mice that was cultured with LPS and IL-4 for 3 days. The arrowhead shows specific band of AID protein. (C) Papilloma frequency after birth in HPV8(+)AID$^{-/-}$ and

HPV8(+)AID$^{+/+}$ mice. (D) HE staining of skin tissues from HPV8(+)AID$^{+/+}$ and HPV8(+)AID$^{-/-}$ mice.

Supplementary Informations

Plasmid

pEF1α-HCVcore-iresZsGreen1, for expression of the HCV core protein and ZsGreen1 was generated by cloning cDNA fragment of HCV core gene (genotype1b-Takeuchi *et al.*,1990) into the *Eco*R1-*Bam*H1 sites of pEF1α-IRES ZsGreen1 (Clontech, CA94043, USA).

HepG2 cells and transfection

Human hepatoma-derived cell line HepG2 was cultured in DMEM (Gibco-BRL) containing 10% fetal bovine serum. Trans-IT LT1 transfection reagent (Mirus bio corporation, Madison, WI, USA) was used for pEF1α-HCVcore-iresZsGreen1 transfection. Briefly, one day before transfection, 0.5×10^6 cells were plated and transfected following manufacturer's instruction. 24 hours after transfection, the cells were treated with or without TNFα (100 ng/ml, Sigma-Aldrich, St. Louis, USA) and finally used for RNA extraction.

BL2-AIDER cells

Human B cell lymphoma-derived BL2 cells was stably transfected by AID-ER (estrogen receptor) fusion protein plasmid.

Naïve or stimulated spleen cells

Spleen of 12 months-aged HCV-Tg was gently grilled and pushed through

metal mesh to prepare single cell suspension (naïve spleen cells). A part of them was further cultured in RPMI containing 10%FBS, penicillin/streptomycin, LPS (Sigma-Aldrich, St. Louis, USA) and IL-4 (eBioScience San Diego, USA) to induce AID expression (stimulated spleen cells).

References for Supporting Informations

(Plasmid) Takeuchi, K., Kubo, Y., Boonmar, S. et al. 1990. Nucleotide sequence of core and envelope genes of the hepatitis C virus genome derived directly from human healthy carriers. *Nucl Acids Res* 18:4626

(Supplementary Table 2) Takai, A., Marusawa, H., Minaki, Y. et al. 2012. Targeting activation-induced cytidine deaminase prevents colon cancer development despite persistent colonic inflammation. *Ongogene* 31:1733.

Supplementary Table 1. PCR primers used for mouse genotyping

Primers	Nucleotide sequences
CRE_fP33	CGGCATGGTGCAAGTTGAATAAC
CRE_rP34	CTAACCAGCGTTTTCGTTCTGC
ROSA_HL15	AAGACCGCGAAGAGTTTGTCC
ROSA_HL54	TAAGCCTGCCCAGAAGACTCC
ROSA_HL152	AAGGGAGCTGCAGTGGAGTA
HCV core-F	GCCCACAGGACGTTAAGTTC
HCV core-R	TAGTTCACGCCGTCCTCCAG
HPV8-F	CAATTTTCCTAAGCAAATGGAC
HPV8-R	CACTACATTCAGCTTCCAAAATACA

Supplementary table 2. PCR Primers utilized in RT-PCR

Primers	Nucleotide sequences
IL-4-171S	AACGAGGTCACAGGAGAAGG
IL-4-293AS	AAATATGCGAAGCACCTTGG
IL-13-227S	CAGCATGGTATGGAGTGTGG
IL-13-347AS	ACAGAGGCCATGCAATATCC
TGF-β-1392S	CAACAATTCCTGGCGTTACC
TGF-β-1513AS	CCTGTATTCCGTCTCCTTGG
CD40-L-391S	AGCGAAGCCAACAGTAATGC
CD40-L-490AS	GCTGTTTCCCATTTTCAAGC
Albumin-627S	CAGAGGCTGACAAGGAAAGC
Albumin-808AS	TTCTGCAAAGTCAGCATTGG
CD19-1165S	AAATCCACGCATTCAAGTCC
CD19-1334AS	TCTCATAGCCACTCCCATCC
AID-96S	GGACAGCCTTCTGATGAAGC
AID-196AS	TCTTCACCACGTAGCAGAGG
IL-1-β-316S	CCTTCCAGGATGAGGACATGAG
IL-1-β-462AS	GTTGTTCATCTCGGAGCCTGTAG
(the primers are following the previous report by Takai et al, 2012.)	
18S rRNA-S	TAGAGTGTTCAAAGCAGGCCC
18S rRNA-AS	CCAACAAAATAGAACCGCGGT
TNF-α-181S	GACGTGGAACTGGCAGAAGAG
TNF-α-325AS	CGATCACCCCGAAGTTCAGTAG
IFN-g-133S	GCTTTGCAGCTCTTCCTCATG
IFN-g-282AS	TTGCCAGTTCCTCCAGATATCC
IL-6-57S	TCCATCCAGTTGCCTTCTTG
IL-6-221AS	CCACGATTTCCCAGAGAACA
IL-12-419S	GCCAGTACACCTGCCACAAAG
IL-12-566AS	CCGGAGTAATTTGGTGCTTCA

Supplementary Table 3

A Definitive cell number corresponding to Fig. 2A

	Liver						Splenocytes	
	IHICs							
	B6		HCV(+) AID		HCV(+) AID		HCV(+)AID$^{+/+}$	
	CD11b/B220	CD4/CD8	CD11b/B220	CD4/CD8	CD11b/B220	CD4/CD8	CD11b/B220	CD4/CD8
Upper left	506	2132	609	2040	810	2127	471	1617
Lower left	4505	3472	4805	4295	4967	4166	2602	5924
Upper right	51	39	154	47	285	82	843	40
Lower right	1685	82	2314	1657	1838	1296	4607	717
Total	6747	5725	7882	8039	7900	7671	8523	8298

B Definitive cell number corresponding to Fig.2B

	Liver										
	IHICs						Hepatocytes			Splenocytes	
	B6		AIDcre/RFP HCV(-)		AIDcre/RFP HCV(+)		B6	AIDcre/RFP HCV(-)	AIDcre/RFP HCV(+)	AIDcre/RFP	
	SSC/RFP	B220/RFP	SSC/RFP	B220/RFP	SSC/RFP	B220/RFP	SSC/RFP	SSC/RFP	SSC/RFP	SSC/RFP	B220/RFP
Upper left	4	1542	0	2805	0	3129	5981	6487	6008	0	4367
Lower left	6392	4704	5830	3046	6916	3714	0	0	0	7121	2532
Upper right	5	6	0	222	0	207	0	6	2	0	414
Lower right	6	30	253	60	258	76	0	0	0	532	105
Total	6407	6282	6083	6133	7174	7126	5981	6493	6010	7653	7418

Supplementary Table 4. Skin tumor incidence in HPV8-Tg mice

AID genotype	Total mouse number	Skin tumor	Death	
			Tumor-related	Unknown reason
$AID^{-/-}$	49	15	2	4
$AID^{+/+}$	51	16	1	2

Supplementary Figure Legends

Supplementary Fig. 1 Western blot analysis of HCV core protein expression in the liver of HCV(+) transgenic 12-month-old mice. The HCV proteins were detected by an anti-mouse-HCV core protein monoclonal antibody (upper panel). Whole liver lysate (30 μg) was loaded in each well. An anti-α tubulin antibody (lower panel) was used for the loading control. The positive control was a lysate of HepG2 cells over-expressing the HCV core protein. The Western blot shown is representative of 3 independent experiments.

Supplementary Fig. 2 qRT-PCR measurements of the AID transcripts referred to in Fig.1A, compared to naïve spleen. Each data shows the AID expression in the individual mouse and error bars show standard deviation from triplicate wells of 1 PCR reaction.

Supplementary Fig. 3 Comparison of AID expression in spleen cells, HepG2 cells, and BL2-AIDER cells, and sensitivity of the MAID-2 antibody. (A) AID expression in a serially diluted BL2-AIDER extract (two fold dilution). Endogenous AID (lower band) and exogenous AID-ER were

detected using the MAID-2 antibody. Exogenous AID-ER served as a loading control (upper band) and was ~3 times more concentrated than endogenous AID (measured by Image J (NIH) software). (B) AID expression in naïve spleen cells and a serially diluted extract from spleen cells stimulated with IL-4 and LPS for 3 days (five fold dilution). The MAID-2 antibody detects the C-terminal regions of both human and mouse AID. (C) qRT-PCR analysis using a primer set that amplifies both human and mouse AID mRNAs. AID expression levels in spleen cells (from 12-month-old HCV-Tg mice, naïve or stimulated as above), HepG2 cells (transfected with HCV core plasmid, with or without TNF-α treatment), and BL2-AIDER cells are shown. Because the primers used can amplify both exogenous and endogenous AID, which were present at a 3:1 ratio, 25% of the total q-PCR signal corresponds to the endogenous AID signal. The AID expression values are shown relative to the q-PCR signal obtained with 500 ng RNA from naive spleen cells (*). See Supplementary Information for details. Error bars show standard deviation from duplicate wells of 1 PCR reaction.

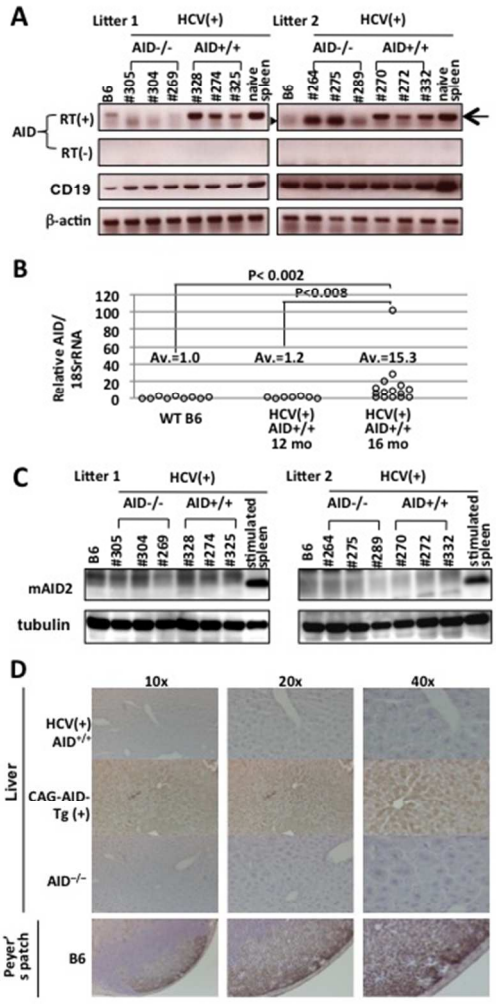

Fig.1 Tung et al.

254x285mm (72 x 72 DPI)

Fig.2 Tung et al.

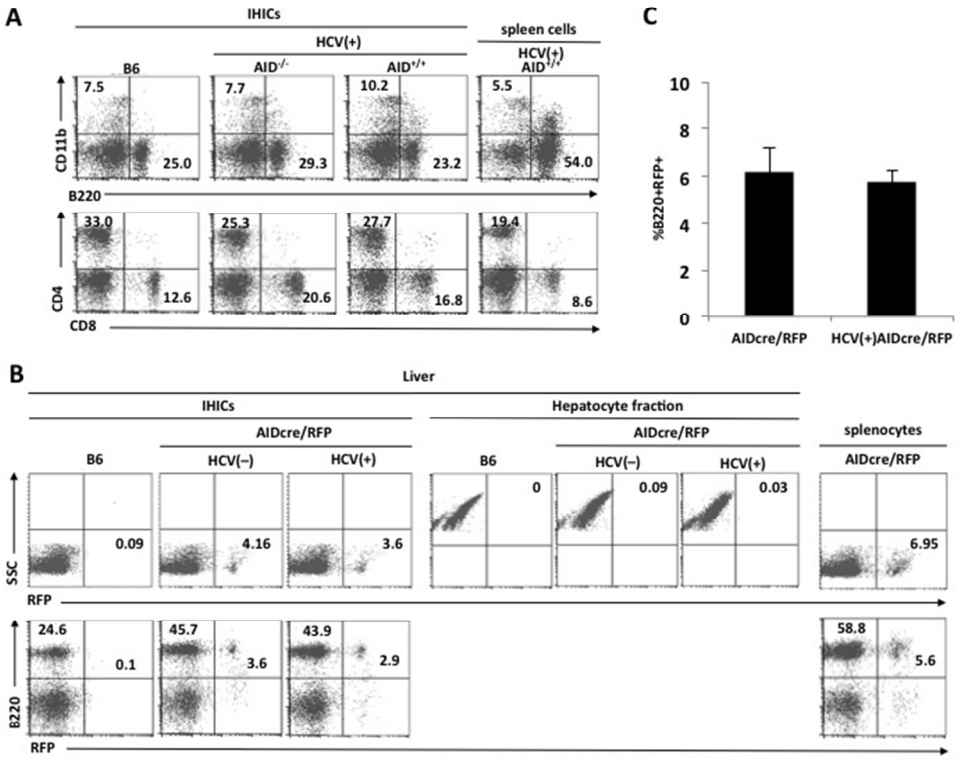

254x285mm (72 x 72 DPI)

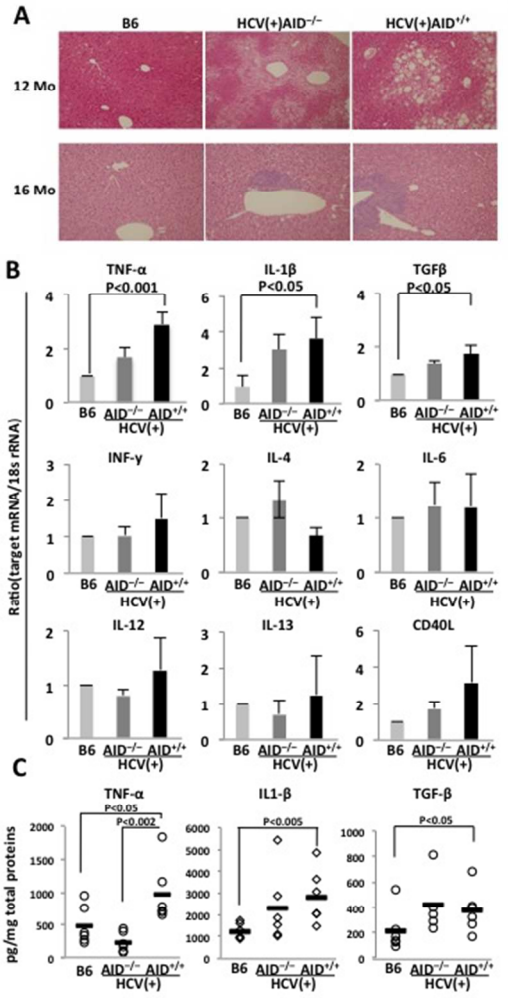

Fig.3 Tung et al.

254x285mm (72 x 72 DPI)

Fig.4 Tung et al.

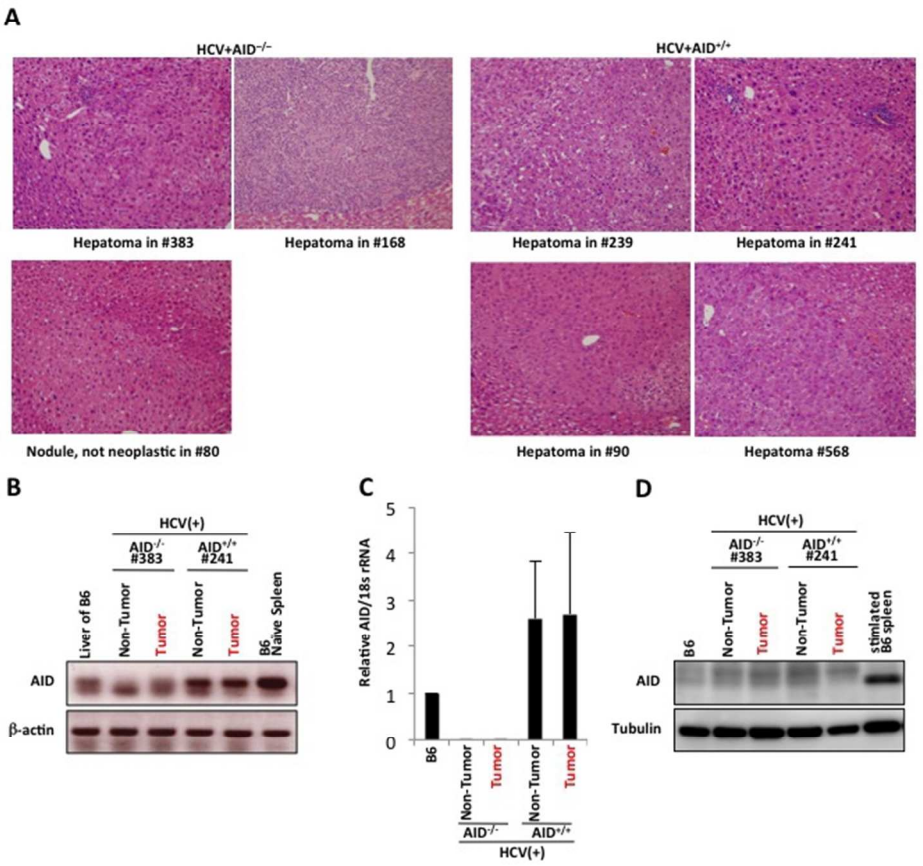

254x285mm (72 x 72 DPI)

Fig.5 Tung et al.

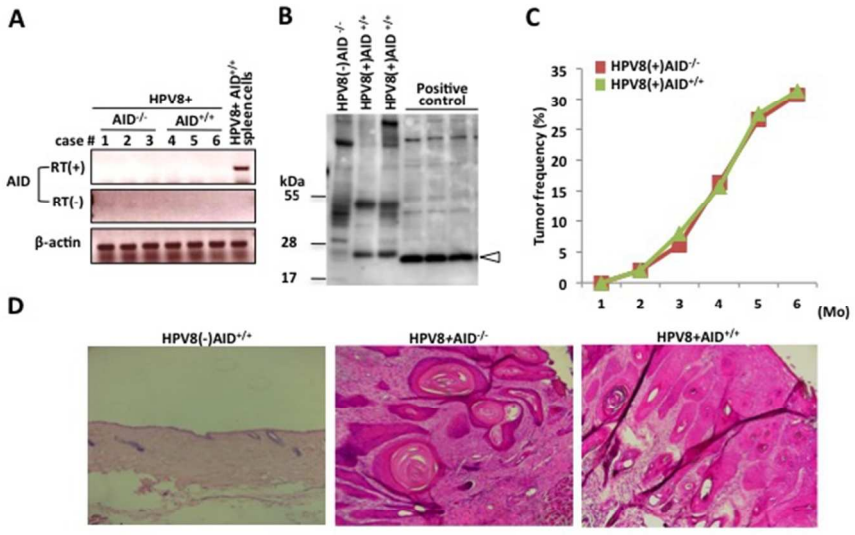

254x285mm (72 x 72 DPI)

Supple.Fig.1 Tung et al.

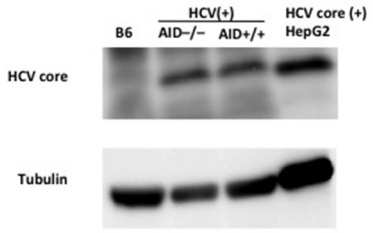

254x285mm (72 x 72 DPI)

Supple.Fig.2 Tung et al.

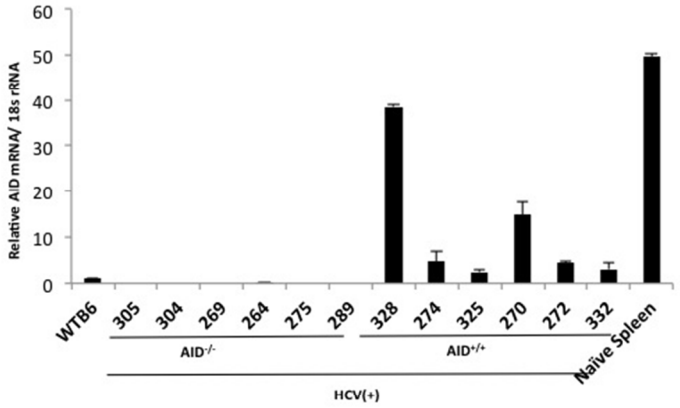

254x285mm (72 x 72 DPI)

Supple.Fig.3 Tung et al.

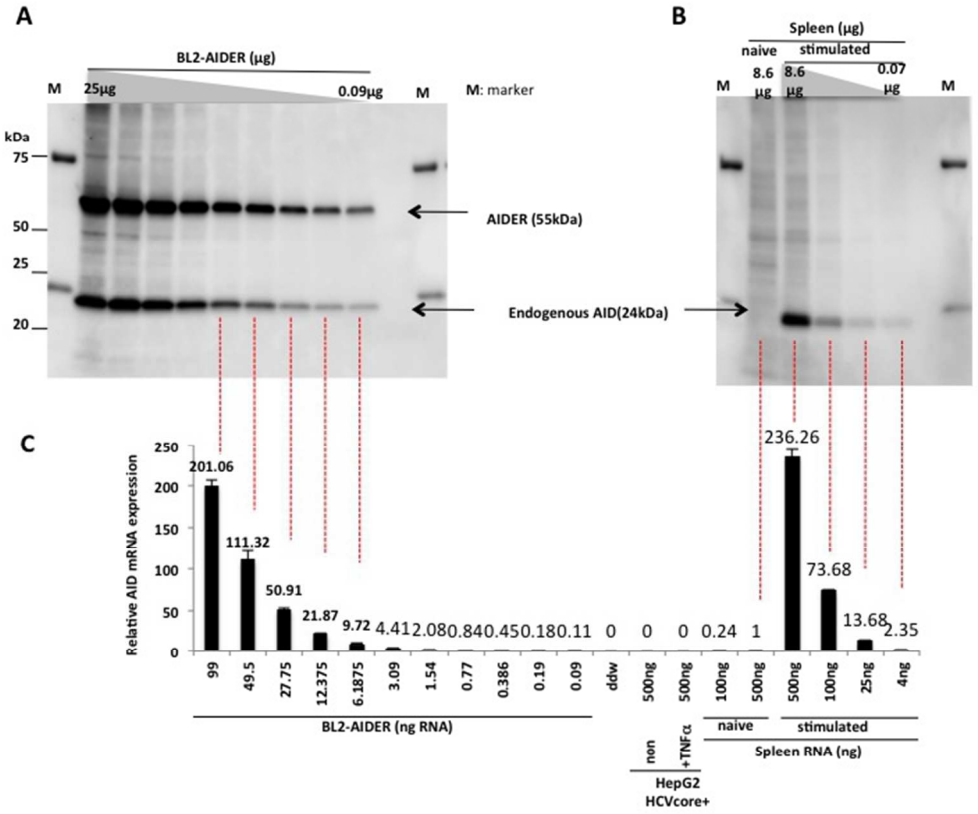

254x285mm (72 x 72 DPI)